Program Digest, 2019 IEEE International Ultrasonics Symposium (IUS)
Glasgow, Scotland, October 6-9, 2019

Low-cost Sensor-enabled Freehand 3D Ultrasound

Carl Herickhoff
Department of Radiology
Stanford University
Stanford, CA, USA
cdh1@stanford.edu

Junhong Lin
Department of Electronic and Information Engineering
Huazhong University of Science and Technology
Hubei, China
junhonghust@hust.edu.cn

Jeremy Dahl
Department of Radiology
Stanford University
Stanford, CA, USA
jjdahl@stanford.edu

***Abstract*—Volumetric 3D ultrasound provides intuitive visualization and spatial context, but most implementations are expensive, using a sophisticated probe design or a cumbersome position-tracking setup requiring calibration. In this work, we implemented freehand 3D ultrasound using low-cost sensors. A custom probe attachment with a pivoting head was made to accommodate IMUs and optical surface-tracking sensors, plus a microcontroller with USB connection. An external laptop with a custom graphical user interface synchronously acquired sensor data and 2D ultrasound images using a Siemens 9L4 probe (depth = 4 cm) and S2000 scanner with a video capture device. Sensor data was stabilized with a gradient descent orientation filter and used to reconstruct a 3D image volume from 500 2D frames, acquired over an irregular path in an abdominal phantom over 15 seconds. The 3D reconstruction time was 30 seconds, and the quality of the 3D image volume was comparable to that of the raw 2D images. These results demonstrate that freehand 3D ultrasound can be practically achieved using low-cost sensors.**

Keywords*—*freehand 3D ultrasound, low-cost, sensors

I. Introduction

As a diagnostic medical imaging modality, ultrasound has several unique advantages over X-ray CT and MRI [1-3]. Ultrasound is comparatively safe (does not involve ionizing radiation or high magnetic fields), fast (acquisition rates >30 frames/sec), and less costly. In addition, ultrasound arrays and probes can be readily designed into many different form factors to optimally image specific targets in the body, and scanners can be made to be very portable, with a number of hand-held systems being released in recent years.

However, conventional ultrasound imaging also has several limitations and challenges. Ultrasound images are most commonly acquired with a hand-held probe, such that there is no common external reference frame as in CT and MRI systems (translating a patient bed through a bore); thus, effective use of ultrasound requires operator skill and training to acquire and interpret images, and operator dependence (inter-operator variability) remains an issue [4-6]. Furthermore, most ultrasound probes consist of one-dimensional arrays to acquire 2D images, which cannot completely capture complex 3D structures in the body. Specialized mechanical 'wobbler' and matrix-array probes have been developed to acquire 3D ultrasound, but the hardware and systems required tend to be complex and expensive.

Work supported by a Wallace H. Coulter Translational Research Grant

Freehand 3D ultrasound has been previously accomplished using precision electromagnetic or optical systems to track a 2D imaging probe and reconstruct a 3D volume [7-9], though these systems are commonly expensive, limited (due to field distortions or obstructed line-of-sight, or in terms of available workspace), and/or require calibration that may be cumbersome. Low-cost sensors, such as an inertial measurement unit (IMU) and optical mouse surface-tracking sensors, have been used in the past to implement 5 degree-of-freedom freehand 3D ultrasound, by rigidly fixing them to an ultrasound probe [10-12]. These implementations have noted error such as bias and drift in inertial and/or optical measurements, thus there is a need for a more flexible and robust approach to low-cost freehand 3D ultrasound.

In this work, we expand on previous 3D ultrasound efforts [13-16], and present an approach to improve the robustness, stability, and ease-of-use for freehand 3D ultrasound via low-cost sensors.

II. Methods

A. Theory

IMUs commonly contain a 3-axis accelerometer, a 3-axis gyroscope, and 3-axis magnetometer, and output orientation information in the form of a unit quaternion. The general form of a quaternion is a scalar, q_0, followed by a vector, $\boldsymbol{q} = (q_1, q_2, q_3)$:

$$q = q_0 + q_1\hat{\boldsymbol{\imath}} + q_2\hat{\boldsymbol{\jmath}} + q_3\hat{\boldsymbol{k}} = q_0 + \boldsymbol{q}$$

Given an axis defined by the vector $\boldsymbol{u} = u_1\hat{\boldsymbol{\imath}} + u_2\hat{\boldsymbol{\jmath}} + u_3\hat{\boldsymbol{k}}$, a quaternion can represent a rotation about $\boldsymbol{u}$ by angle θ as:

$$q = \cos\frac{\theta}{2} + \left(u_1 \sin\frac{\theta}{2}\right)\hat{\boldsymbol{\imath}} + \left(u_2 \sin\frac{\theta}{2}\right)\hat{\boldsymbol{\jmath}} + \left(u_3 \sin\frac{\theta}{2}\right)\hat{\boldsymbol{k}}$$

$$q = \cos\frac{\theta}{2} + \sin\frac{\theta}{2}\boldsymbol{u}$$

Also, the transformation of a vector $\boldsymbol{v}$ as a rotation of θ about $\boldsymbol{u}$ can be represented according to the following operation with unit quaternion q:

$$\boldsymbol{v}' = q\boldsymbol{v}q^*$$

where $q^* = q_0 - \boldsymbol{q}$ is the quaternion conjugate. If, in some local coordinate system, one or more optical trackers sense an incremental translation of x_s and y_s over a surface while an IMU senses an orientation quaternion of q, this can be transformed into translations in the global coordinate system as:

$$\Delta x = x_s \cdot [\cos\theta + (1-\cos\theta)u_1{}^2] + y_s \cdot [(1-\cos\theta)u_1 u_2 - u_3 \sin\theta]$$

$$\Delta y = x_s \cdot [(1-\cos\theta)u_1 u_2 + u_3 \sin\theta] + y_s \cdot [\cos\theta + (1-\cos\theta)u_2{}^2]$$

$$\Delta z = x_s \cdot [(1-\cos\theta)u_1 u_3 - u_2 \sin\theta] + y_s \cdot [(1-\cos\theta)u_2 u_3 + u_1 \sin\theta]$$

B. Approach and Hardware Design

In order to better de-couple the surface and position tracking from the probe orientation tracking, an attachment to a handheld linear-array ultrasound probe (Siemens 9L4) was designed with a pivoting base at the head of the probe. The base was designed to accommodate two small custom printed circuit boards (PCBs), vertically-oriented to enable compact packaging. Each of these base PCBs housed a right-angle optical sensor (PixArt Imaging, Hsinchu, Taiwan) at the bottom edge to track translation over the body surface, and one also contained a surface-mount IMU (STMicroelectronics, Geneva, Switzerland). The separation of the two optical sensors allowed the detected surface translation (x_s and y_s) to be averaged, such that rotation about one sensor would not give a spurious reading; thus a robust estimate of the global x,y,z translation of the center of the base could be obtained (as derived in section II.A.).

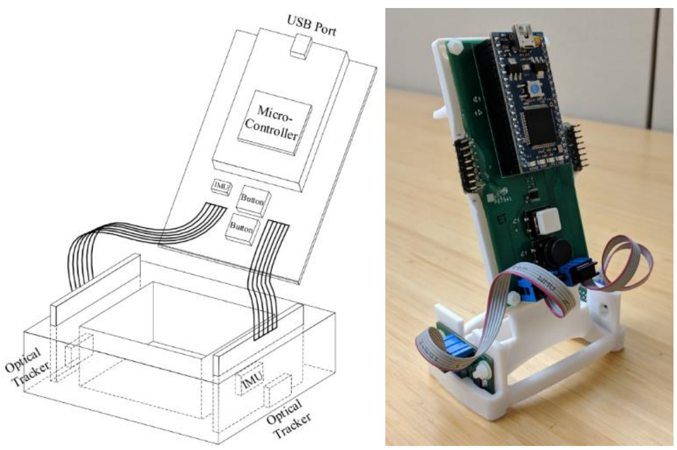

Fig. 1. Schematic of low-cost sensor layout (left) and completed probe attachment prototype with mounted base and body PCBs (right).

Another, larger custom PCB was mounted to the body of the probe attachment; this body PCB contained an IMU, two push buttons for user control input, and an mbed microcontroller (NXP Semiconductors, Eindhoven, The Netherlands) with a USB interface. An external laptop was connected to the microcontroller via USB to provide power, pre-program routines, and stream data. Both small base PCBs were connected to the body PCB and microcontroller via a 6-conductor ribbon cable, such that both optical sensors (on the base) and both IMUs (on the base and the body PCB) were powered by and provided digital data to the microcontroller (I^2C interface) and laptop (via a serial port).

The external laptop was also connected via USB to a video capture device (Epiphan Systems, Palo Alto, CA, USA) to obtain real-time 2D ultrasound image input from the external display port of a Siemens S2000 scanner. The streaming video was automatically cropped to the rectangular area representing the imaging frame. Thus 2D image data and probe trajectory and pose data could be synchronously acquired—during a sweep of the probe over the surface of the body—and used as input to a 3D image reconstruction process.

C. System Software Implementation

Empirical observation of raw magnetometer measurements (m_x,m_y,m_z) revealed data points distributed on a biased ellipsoid rather than a sphere centered at the origin, thus an ellipsoid-fitting compass calibration method was implemented on the laptop to re-scale the ellipsoid to a sphere and determine and compensate for the center offset. Output of this calibration routine was stored on the microcontroller to correct distortion of magnetic field measurements. In addition, to stabilize and reduce drift in quaternion measurements from the two IMUs, a gradient descent orientation filter, as described by Madgwick, et al. [17], was implemented in software embedded on the microcontroller.

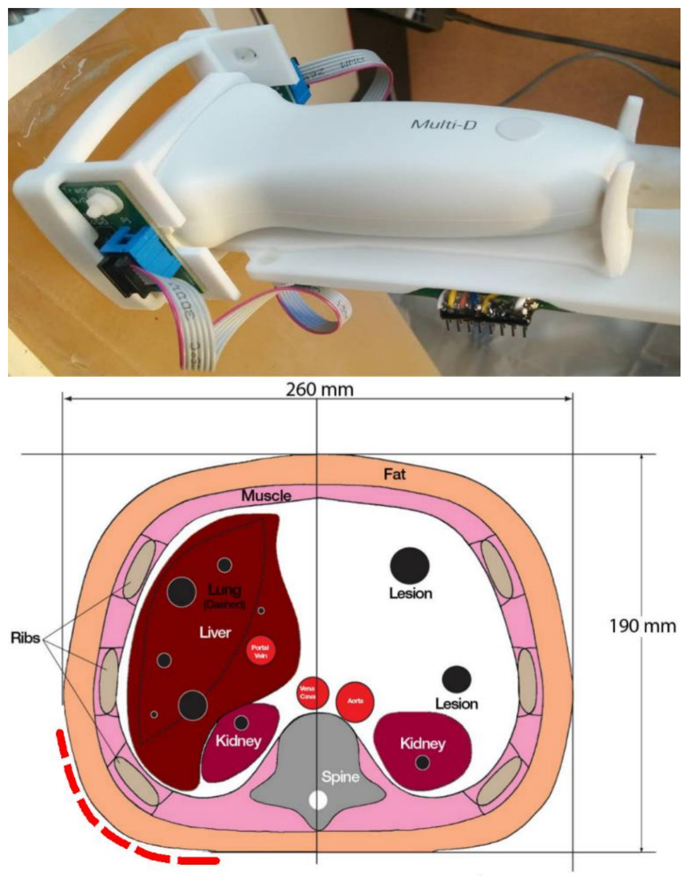

Fig. 2. Siemens 9L4 probe with attachment prototype (top) and schematic of CIRS 057A phantom (bottom; red dashed line indicates approximate path of probe during acquisition sweep).

In order to synchronize acquisition of a 2D ultrasound image frame and the IMUs and optical sensors, a multi-threaded routine was implemented on the laptop. First, a request was simultaneously sent to both the video capture device and the microcontroller; the IMU quaternion data was then filtered on the microcontroller until a 2D video frame was returned, at which point the 2D frame and (latest, filtered) quaternion data and optical track sensor data were saved. An acquisition sweep was considered complete when 500 2D frames were captured.

The 3D trajectory of the center of the attachment base in the global reference frame was found by averaging the (x_s,y_s) readings from the optical sensors and combining with the base IMU data, as previously described. At each point in this trajectory, two offsets were applied—in directions given by each IMU—to determine the appropriate location of each 2D image for 3D reconstruction: (1) the distance from the bottom of the base (i.e., the patient's skin surface) to the attachment pivot axis between the base and body, according to the orientation from the base IMU, and (2) the distance from the pivot axis to the face of the transducer (i.e., the top edge of the image), according to the orientation from the body IMU. With the position of each 2D image determined, a pixel-based reconstruction algorithm was used to assign pixel data to a voxel grid.

A custom graphical user interface (GUI) was developed using the Win32 API on the laptop to guide calibration and acquisition. The GUI allowed the user to adjust input parameters such as video cropping, surface-to-axis and axis-to-transducer distances, and pixel or voxel spacing. The GUI displayed the live video feed from the ultrasound scanner, and after an acquisition sweep and reconstruction process was completed, the GUI also used Open GL to display the calculated 3D trajectory of the probe attachment base and the reconstructed 3D image in separate viewing windows. The 3D image was displayed with opacity corresponding to voxel intensity.

D. Freehand 3D Ultrasound: Phantom Experiment

The completed low-cost freehand 3D ultrasound system was used to perform a volumetric acquisition on an abdominal phantom (CIRS Model 057A). The transducer and image plane were swept by hand over a curved surface of the phantom, at an approximate speed of 1.0 ± 0.25 cm/sec, and the 3D trajectory and 3D image volume were computed.

III. Results

The 3D trajectory and 3D image volume were reconstructed in 30 seconds, with output shown in Fig. 3. Edges of the liver and kidney structures embedded in the phantom are visible, though a significant region is obscured due to shadowing from an overlying rib. A defect near one edge of the phantom resulted in a reverberation artifact seen as multiple equally-spaced layers. At one point there appears to be a gap in the outer region of the image due to the probe being swept faster than the video capture could acquire 2D image data.

IV. Discussion

Our approach to freehand 3D ultrasound via low-cost sensors differs from previous implementations by utilizing multiple IMUs and a pivoting base at the head of the probe attachment. In addition, our use of right-angle optical sensors allowed PCBs in the base to be oriented vertically, enabling packaging that was relatively compact overall. Calibration of the IMU's magnetometer and use of a gradient descent filter on the unit quaternion output gave improved accuracy and stability to orientation measurements, allowing the 3D path and 3D image volume to be reliably reconstructed. The quality of obtained 3D image volumes was considered comparable to the 2D image quality obtained from the scanner, and reconstruction time of 30 seconds was considered acceptable.

Fig. 3. (top) GUI implementation showing reconstructed 3D path and 3D image volume; (bottom) reconstructed 3D image volume showing edges of liver and kidney shadowed by rib, with shallow reverberation artifact.

Ultrasound imaging with handheld probes is inherently operator dependent, but fast and easy freehand 3D acquisitions properly oriented with respect to the patient could reduce inter-operator variability and reduce the level of skill and training necessary to obtain clinically useful images. These initial results show the practicality of our low-cost sensor-based approach to freehand 3D ultrasound, and suggest that direct integration of such sensors and methods into commercial probes and systems could significantly expand the use of 3D ultrasound for a variety of clinical applications.

Acknowledgment

This work was funded by a Stanford-Coulter Translational Research Award by the Wallace H. Coulter Foundation

REFERENCES

[1] C. D. Herickhoff, M. R. Morgan, J. S. Broder, and J. J. Dahl, "Low-cost volumetric ultrasound by augmentationof 2d systems: Design and prototype," Ultrasonic imaging, vol. 40, no. 1, pp. 35–48, 2018.

[2] M. R. Morgan, J. S. Broder, J. J. Dahl, and C. D. Herickhoff, "Versatile low-cost volumetric 3-d ultrasound platform for existing clinical 2-d systems," IEEE transactions on medical imaging, vol. 37, no. 10, pp. 2248–2256, 2018.

[3] E. Picano, "Sustainability of medical imaging,"Bmj, vol. 328, no. 7439, pp. 578–580, 2004.

[4] M. G. Tolsgaard, C. Ringsted, E. Dreisler, L. N. Nørgaard, J. H. Petersen, M. E. Madsen, N. L. Freiesleben,J. L. Sørensen, and A. Tabor, "Sustained effect of simulation-based ultrasound training on clinical performance: a randomized trial," Ultrasound in Obstetrics & Gynecology, vol. 46, no. 3, pp. 312–318, 2015.

[5] R. Ahmad, G. Alhashmi, A. Ajlan, and B. Eldeek, "Impact of high-fidelity transvaginal ultrasound simulationfor radiology on residents' performance and satisfaction," Academic radiology, vol. 22, no. 2, pp. 234–239,2015.

[6] F. P. Glor, B. Ariff, A. D. Hughes, P. R. Verdonck, S. M. G. Thom, D. C. Barratt, and X. Y. Xu, "Operator dependence of 3-d ultrasound-based computational fluid dynamics for the carotid bifurcation," IEEE transactions on medical imaging, vol. 24, no. 4, pp. 451–456, 2005.

[7] R. W. Prager, U. Z. Ijaz, A. Gee, and G. M. Treece, "Three-dimensional ultrasound imaging," Proceedings of the Institution of Mechanical Engineers, Part H: Journal of Engineering in Medicine, vol. 224, no. 2, pp.193–223, 2010.

[8] O. V. Solberg, F. Lindseth, H. Torp, R. E. Blake, and T. A. N. Hernes, "Freehand 3d ultrasound reconstruction algorithms: a review, "Ultrasound in medicine & biology, vol. 33, no. 7, pp. 991–1009, 2007.

[9] A. Lasso, T. Heffter, A. Rankin, C. Pinter, T. Ungi, and G. Fichtinger, "Plus: open-source toolkit for ultrasound-guided intervention systems," IEEE Transactions on Biomedical Engineering, vol. 61, no. 10, pp. 2527–2537, 2014.

[10] A. Goldsmith, P. Pedersen, and T. Szabo, "An inertial-optical tracking system for portable, quantitative, 3dultrasound," in Ultrasonics Symposium, 2008. IUS 2008. IEEE. IEEE, 2008, pp. 45–49.

[11] P. J. Stolka, J. Choi, J. Wang, M. Choti, and E. M. Boctor, "5-dof trajectory reconstruction for handheld ultrasound with local sensors," inUltrasonics Symposium (IUS), 2009 IEEE International. IEEE, 2009, pp.1864–1867.

[12] P. J. Stolka, X. L. Wang, G. D. Hager, and E. M. Boctor, "Navigation with local sensors in handheld 3d ultra-sound: initial in-vivo experience," inSPIE Medical Imaging. International Society for Optics and Photonics,2011, pp. 79 681J–79 681J.

[13] C. Herickhoff, M. Morgan, J. Broder, and J. Dahl, "Low-cost 3d ultrasound with any probe: A sensor-based approach," in Ultrasonics Symposium (IUS), 2017 IEEE International. IEEE, 2017, pp. 1–1.

[14] J. Broder, E. Jaffa, M. Morgan, C. Herickhoff, B. Smith, E. Peethumnongsin, and J. Dahl, "394 brain imagingusing a novel three-dimensional ultrasound system,"Annals of Emergency Medicine, vol. 70, no. 4, pp.S154–S155, 2017.

[15] M. R. Morgan, C. D. Herickhoff, J. S. Broder, and J. J. Dahl, "Low cost 3d doppler ultrasound: Preliminary invivo results," in Ultrasonics Symposium (IUS), 2017 IEEE International. IEEE, 2017, pp. 1–1.

[16] J. Broder, E. Jaffa, T. Irons, E. Peethumnongsin, R. Theophanous, A. Limkakeng, J. Vissoci, M. Morgan,C. Herickhoff, and J. Dahl, "212 3d volume ultrasound of the right lower quadrant for diagnosis of appendici-tis," Annals of Emergency Medicine, vol. 72, no. 4, p. S85, 2018.

[17] S. O. Madgwick, A. J. Harrison, and R. Vaidyanathan, "Estimation of imu and marg orientation using agradient descent algorithm," in 2011 IEEE international conference on rehabilitation robotics. IEEE, 2011, pp. 1–7.